# Future Prediction of Consecutive Dry Days (CDD) in Rapti River Basin using Model ACCESS-CM2 Climate Projection


## ABSTRACT

The Rapti River basin in India is a region increasingly vulnerable to extreme precipitation events, which pose significant challenges to water resource management and flood mitigation. This study investigates the extreme precipitation patterns in the Rapti River Basin, India, by analyzing historical and projected data using advanced climate models and indices. Utilizing the Expert Team on Climate Change Detection and Indices (ETCCDI) framework, we focus on Consecutive Dry Days (CDD). The study evaluates the trends under different global warming scenarios of 1.5˚C, 2˚C, and 3˚C, employing ACCESS-CM2 Model.The findings reveal significant variations in the trends and magnitudes of CDD across the different warming levels. At 1.5˚C, CDD shows a decreasing trend. At 2˚C, models project a continued decrease in CDD. At 3˚C, mixed trends are observed with notable increases in CDD, highlighting the potential for prolonged wet periods and increased flood risks. The study underscores the impact of climate change on the hydrological behavior of the Rapti River Basin, emphasizing the need for adaptive water resource management strategies. It provides valuable insights into the future precipitation trends in the Rapti River Basin, guiding the development of strategies to enhance resilience against climate-induced hydrological changes.



***Keywords****: Consecutive Dry Days, Rapti River Basin, climate Projection, ETCCDI Indices*




## 1. INTRODUCTION

The increasing impact of climate change on hydrological systems is a critical concern for water resource management, agriculture, and environmental sustainability. The Rapti River Basin, a significant tributary of the Ghaghara River in northern India, has been experiencing frequent extreme weather events, particularly prolonged dry periods, known as Consecutive Dry Days (CDD). Understanding and predicting these CDD trends under future climate scenarios is essential for developing effective adaptation and mitigation strategies.

Climate change, driven by anthropogenic activities, has led to significant alterations in global weather patterns, including increased frequency and intensity of extreme events **[1]**. The Intergovernmental Panel on Climate Change (IPCC) projects that with rising global temperatures, the variability and intensity of precipitation events will become more pronounced **[2]**. This has significant implications for regions like the Rapti River Basin, where agriculture and livelihoods are heavily dependent on consistent and predictable rainfall patterns.

Recent studies have highlighted the importance of modeling climate impacts on hydrological processes to understand future risks and inform policy decisions **[3; 4]**. Process-based models, such as the Soil and Water Assessment Tool (SWAT), have been widely used to simulate the effects of climate change on water resources **[5]**. However, the application of climate projection models, such as ACCESS-CM2, provides a more detailed and localized understanding of future climate scenarios.
The Rapti River Basin has been prone to both droughts and floods, with historical records indicating severe flooding events in 1992, 1998, 2000, 2008, 2014, 2017, 2018, 2019, and 2020 **[6]**. These events underscore the basin's vulnerability to extreme weather and the necessity for robust predictive models to guide water resource management and agricultural planning. With the projected increase in global temperatures, it is crucial to assess how these changes will influence the occurrence and duration of CDD in the basin.

Therefore, this study aims to understand the rainfall characteristics of the Rapti River Basin. It includes an analysis of daily, seasonal, and annual rainfall using gridded rainfall data for the Rapti Basin. The study also focuses on examining the temporal variability of rainfall with ETCCDI indices, analyzing trends in the gridded rainfall data, and understanding the rainfall characteristics of the basin. Additionally, the research aims to determine the change point in rainfall patterns within the basin and relate this change point to flooding events. The findings indicate that flooding in the basin increases after the identified change point. Gorakhpur, situated in the downstream area of the basin, is the most flood-prone region, despite experiencing the highest number of consecutive dry days. Rainfall in the upstream areas significantly contributes to flooding in Gorakhpur.

This study aims to investigate the variability and trends in extreme precipitation within the Rapti River Basin from the historical data, 1971 to 2014 provided by Indian Meteorological Data, Pune and the projected data, 2015 to 2100 using bias corrected CMIP6 Datasets. By employing an iterative Mann-Kendall trend test, we seek to provide a comprehensive understanding of historical precipitation extremes and their potential future trajectories. Understanding these patterns is crucial for developing effective strategies to mitigate the adverse effects of climate change and to enhance the resilience of the communities dependent on the Rapti River Basin.

## 2. MATERIAL AND METHODS

### 2.1 Study Area

The Rapti River Basin is located primarily in the northern part of India, within the state of Uttar Pradesh. The basin stretches approximately between the latitudes of 26.5°N to 28.5°N and the longitudes of 82.5°E to 84.5°E. In India, the Rapti River flows through several districts including Bahraich, Shravasti, Balrampur, Siddharthnagar, Gorakhpur, and Sant Kabir Nagar. The total area covered by the Rapti River Basin in India is roughly around 30,000 square kilometers. This area is characterized by a mix of agricultural land, forests, and urban settlements, with the river playing a significant role in the region's agriculture and economy **[7]**.

The geography of the Rapti River Basin is diverse, encompassing the Terai plains at the foothills of the Himalayas. This region is known for its fertile soil, making it an important agricultural zone. The terrain is generally flat with some undulating areas, particularly closer to the river. The basin is prone to flooding during the monsoon season due to the flat topography and heavy rainfall**[8, 9].**.

The climate of the Rapti River Basin is predominantly subtropical, with distinct seasons: Summer (March to June): Hot and dry, with temperatures ranging from 30°C to 45°C.
Monsoon (July to September): Marked by heavy rainfall, with the region receiving an average annual precipitation of about 1,200 to 1,500 mm. This period is crucial for replenishing water resources but also brings the risk of floods.
Winter (October to February): Mild and dry, with temperatures ranging from 5°C to 25°C**[10, 11]**.

The temperature in the Rapti River Basin varies significantly with the seasons:
Summer: High temperatures often exceed 40°C during peak periods.
Monsoon: Temperatures are relatively lower than in summer, ranging from 25°C to 35°C, but humidity levels are high.
Winter: Temperatures can drop to around 5°C during the coldest months, with daytime temperatures ranging between 15°C and 25°C.

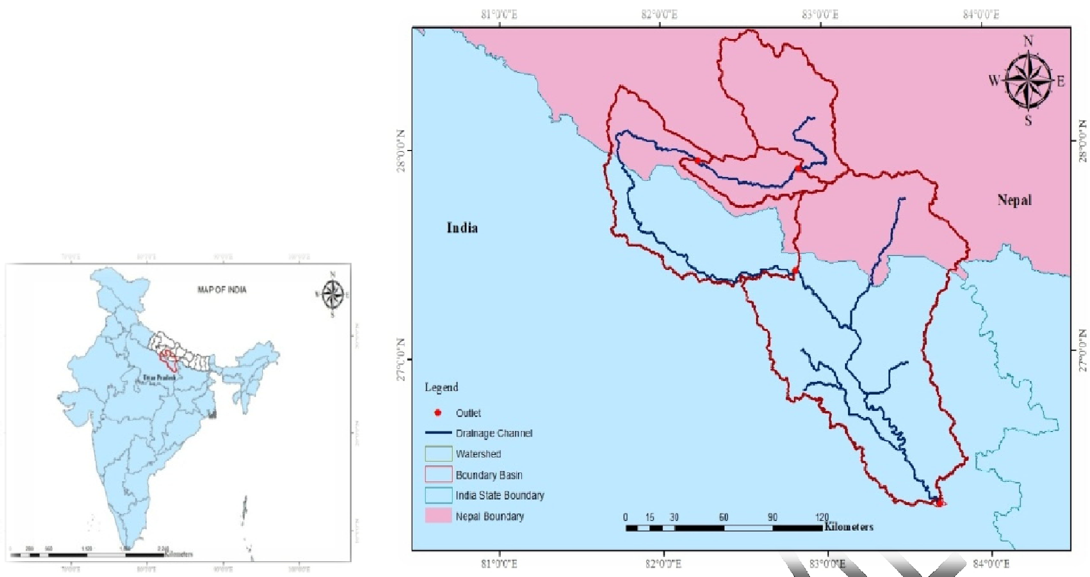


**Figure 1: Location of the study area**

## 2.2 Metreological Data

The rainfall datasets (1971-2014) was collected from the Indian Meteorological Department (IMD), Pune, and the long-term annual data (2015-2100) for CDD, i.e., the maximum annual number of consecutive dry days (when precipitation < 1.0 mm),obtain from Centre for Climate Change Research, Pune were used in this study. The bias-corrected CMIP6 datasets used in the study are available at https://zenodo.org/record/3873998#.Y7xgvnZBy01 for the Indian region at 0.25° × 0.25° grids given by **[12]**.

**Table 1.59 *Stations* located in India and NepalofRapti River basin**

| Stations | Latitude | Longitude | Stations | Latitude | Longitude |
|---|---|---|---|---|---|
| 01 | 26.375 | 83.375 | 31 | 28.375 | 81.625 |
| 02 | 26.375 | 83.625 | 32 | 27.875 | 81.875 |
| 03 | 26.375 | 83.875 | 33 | 28.125 | 81.875 |
| 04 | 26.625 | 83.125 | 34 | 28.375 | 81.875 |
| 05 | 26.625 | 83.375 | 35 | 27.875 | 82.125 |
| 06 | 26.625 | 83.625 | 36 | 28.125 | 82.125 |
| 07 | 26.625 | 83.875 | 37 | 27.875 | 82.375 |
| 08 | 26.875 | 82.625 | 38 | 28.125 | 82.375 |
| 09 | 26.875 | 82.875 | 39 | 28.375 | 82.375 |
| 10 | 26.875 | 83.125 | 40 | 28.625 | 82.375 |
| 11 | 26.875 | 83.375 | 41 | 27.875 | 82.625 |
| 12 | 27.125 | 82.125 | 42 | 28.125 | 82.625 |
| 13 | 27.125 | 82.625 | 43 | 28.375 | 82.625 |
| 14 | 27.125 | 82.875 | 44 | 28.625 | 82.625 |
| 15 | 27.125 | 83.125 | 45 | 27.625 | 82.875 |
| 16 | 27.125 | 83.375 | 46 | 27.875 | 82.875 |
| 17 | 27.125 | 83.625 | 47 | 28.125 | 82.875 |
| 18 | 27.375 | 82.125 | 48 | 28.375 | 82.875 |
| 19 | 27.375 | 82.375 | 49 | 28.625 | 82.875 |
| 20 | 27.375 | 82.625 | 50 | 27.625 | 83.125 |
| 21 | 27.375 | 82.875 | 51 | 27.875 | 83.125 |
| 22 | 27.375 | 83.125 | 52 | 28.125 | 83.125 |
| 23 | 27.375 | 83.375 | 53 | 28.375 | 83.125 |
| 24 | 27.375 | 83.625 | 54 | 27.625 | 83.375 |
| 25 | 27.625 | 81.875 | 55 | 27.875 | 83.375 |
| 26 | 27.625 | 82.125 | 56 | 27.625 | 83.625 |
| 27 | 27.625 | 82.375 | 57 | 27.875 | 83.625 |
| 28 | 27.625 | 82.625 | 58 | 27.375 | 83.875 |
| 29 | 27.875 | 81.625 | 59 | 27.625 | 83.875 |

| | | | | | |
|---|---|---|---|---|---|
| 30 | 28.125 | 81.625 | | | |

### 2.3 Mann- Kendall Test for Trends

The Mann-Kendall test is a non-parametric statistical test used to detect trends in time series data. It is particularly useful for identifying monotonic trends in environmental data, such as precipitation or temperature, without requiring the data to follow a specific distribution. The test is named after **[13 and 14]**, who developed it in the late 20th century.

The Mann-Kendall test statistic (S) is calculated based on the number of positive and negative differences between data points.

For a time series of n data points {x1,x2,...............,xn}:

$$s = \sum_{i=1}^{n-1} \sum_{j=i+1}^{n} sgn\left(x_j - x_i\right) \ldots.(1)$$

Where,

$$sgn\left(x_j - x_i\right) = \begin{Bmatrix} 1\ if\left(x_j - x_i\right) > 0 \\ 0\ if\left(x_j - x_i\right) = 0 \\ -1\ if\left(x_j - x_i\right) < 0 \end{Bmatrix} \ldots.(2)$$

$$VAR(s) = \frac{n(n-1)(2n+5) - \sum_{i=1}^{m} t_i(t_i - 1)(2t_i + 5)}{18} \ldots(3)$$

Where tirepresents the number of data points in the ith tied group, m is the total number of tied groups (a tied or connected group consists of a set of data points with the same value), and n is the total number of data points.

The standard test statistic Z is calculated using the following formula:

$$Z = \begin{cases} \dfrac{s-1}{\sqrt{VAR(s)}}\ ifs > 0 \\ 0\ ifs = 0 \\ \dfrac{s+1}{\sqrt{VAR(s)}}\ ifs < 0 \end{cases} \ldots(4)$$

The statistical significance Z of the test statistics is evaluated at three different levels of significance: 1%, 5%, and 10%. If the time series exhibits a strong lag-1 serial correlation, the Mann-Kendall (MK) test with pre-whitening is employed, as recommended by **[15].**

**Sen's Slope Estimator**

To quantify the magnitude of the trend, Sen's Slope Estimator is often used. It calculates the median slope between all pairs of data points.

$$\beta = Median\left[\frac{x_j - x_i}{j - i}\right] \text{f or all i } < j \ldots(5)$$

Where 1<j<i<n and β is the robust estimate of the trend magnitude. A positive value of β indicates an 'upward trend', while a negative value of β indicates a 'downward trend' (Xu et al., 2007). Xjrepresents the data value at time j, and Xi represents the data value at an earlier time i.

The relative change is calculated using the following equation **[16]**:

$$\mathrm{RC} = \frac{\mathrm{n} * \beta}{|\mathrm{x}|} * 100 \qquad \ldots(6)$$

Where, |x|is the absolute average value of the time series, n is the length of the time series, and β is the trend slope estimated using Sen's median estimator.

## 2.4 Shared Socioeconomic Pathways (SSPs)

Shared Socioeconomic Pathways (SSPs) are a set of scenarios used to model and understand potential future global changes in climate, economics, and society. Developed as part of the framework for climate change research, SSPs help in examining how different societal trends might influence greenhouse gas emissions, climate policies, and adaptive capacities.**[ 17,18].** They are integral to the Coupled Model Intercomparison Project Phase 6 (CMIP6) and are used in conjunction with Representative Concentration Pathways (RCPs) to provide a comprehensive view of possible futures.

SSPs are used in various fields of research and policy-making to explore and plan for future scenarios: SSPs are combined with RCPs to create integrated scenarios that model both socioeconomic and climate changes. This helps in understanding the potential impacts of different levels of greenhouse gas emissions.Researchers use SSPs to assess the impacts of climate change on various sectors, including agriculture, water resources, health, and infrastructure. These assessments help identify vulnerabilities and inform adaptation strategies.

## 2.5 Extreme precipitation Indices

Extreme precipitation indices are quantitative measures used to assess and characterize extreme rainfall events. These indices help in understanding the frequency, intensity, duration, and spatial extent of extreme precipitation, which are crucial for studying climate variability, assessing water resources, and managing risks associated with floods and droughts. Here are some common extreme precipitation indices. The 11 precipitation indices are categorized based on their characteristics into measures of precipitation intensity, frequency, and duration across various precipitation schemes, as outlined in reference **[19].** Using the Expert Team on Climate Change Detection and Indices (ETCCDI) indexes, the characteristics of extreme rainfall are assessed. ETCCDI provided twenty-seven core indices to determine the characteristics of precipitation and temperature **[20].** Among these indices, CDD (Consecutive Dry Days) is used in this study to measure precipitation characteristics. The descriptions of the indices used are provided in Table 2.

**Table 2.Precipitation indices used in this study**

| **Index** | **Precipitation** Duration | **Definition** | **Unit** |
|---|---|---|---|
| CDD | Consecutive Dry Days | Maximum annual number of consecutive dry days (i.e., when precipitation < 1 mm) | days |

## 2.6 Projected changes of precipitation extremes at 1.5 °C , 2 °C and 3°C GWLs

Understanding the projected changes in precipitation extremes at various global warming levels (GWLs) is crucial for anticipating future climate impacts on the Rapti River Basin. The analysis focuses on three key warming thresholds: 1.5°C, 2°C, and 3°C above pre-industrial levels. These projections are based on climate model simulations and provide insights into how increasing global temperatures may alter extreme precipitation patterns in the basin.

**Table 3.Detail of selected Climate Models of CMIP6 for the study**

| **Sr. No.** | **CMIP 6 Model** | ***Description*** | ***Precipitation indices under GWLs*** | | | | | | | | |
|---|---|---|---|---|---|---|---|---|---|---|---|
| | | | ***CDD*** | | | ***CDD*** | | | ***CDD*** | | |
| | | | ***1.5˚C*** | ***2˚C*** | ***3˚C*** | ***1.5˚C*** | ***2˚C*** | ***3˚C*** | ***1.5˚C*** | ***2˚C*** | ***3˚C*** |

| | | | | | | | | | | | |
|---|---|---|---|---|---|---|---|---|---|---|---|
| **1** | **M1** | ACCESS-CM2 | 2020-2031 | 2032 - 2050 | 2051 - 2060 | 2020 - 2031 | 2032 - 2050 | 2051-2060 | 2020-2031 | 2032 - 2050 | 2051-2060 |

## 3. RESULT AND DISCUSSION

### 3.1 Annual Precipitation Extremes

We evaluated four precipitation extremes using Model ACCESS-CM2, under various global warming levels of 1.5˚C, 2˚C, and 3˚C, across multiple time scales.
The range of maximum Consecutive Dry Days (CDD) values at 1.5˚C (2020-2031) varies between 208 days and 49 days for the ACCESS-CM2 Model, ssp 585, with the minimum value ranging from 72 days to 28 days..

The highest CDD value at 2˚C (2032-2050) for ACCESS-CM2 Model, ssp 585, spans between 166 days and 60 days, while the lowest value varies from 102 days to 22 days.

The highest CDD value at 3˚C (2051-2060) for ACCESS-CM2 Model, ssp 585, varies between 136 days and 53 days, with the lowest value ranging from 68 days to 24 days.

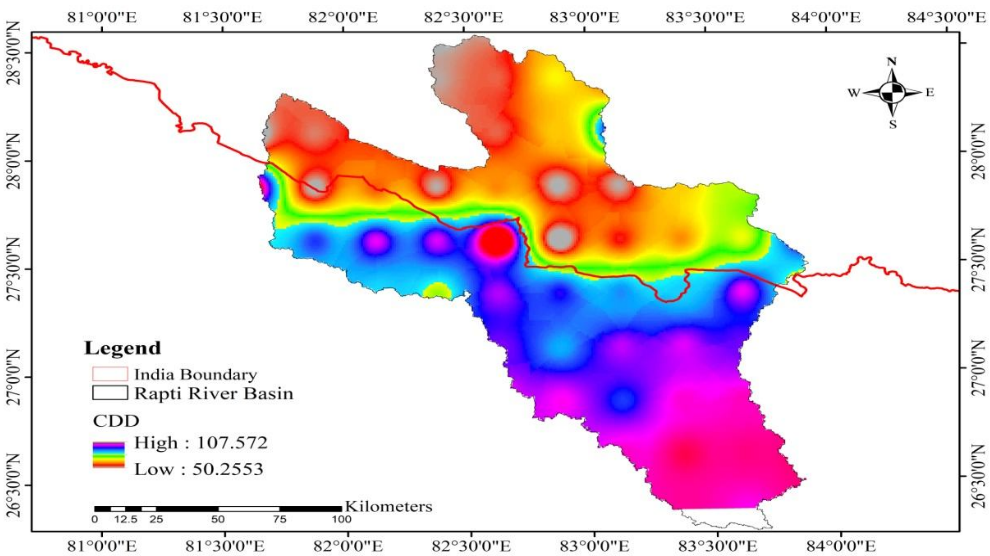


**Figure 2: Consecutive Dry Days (CDD) atACCESS-CM2 Model for 1.5˚**

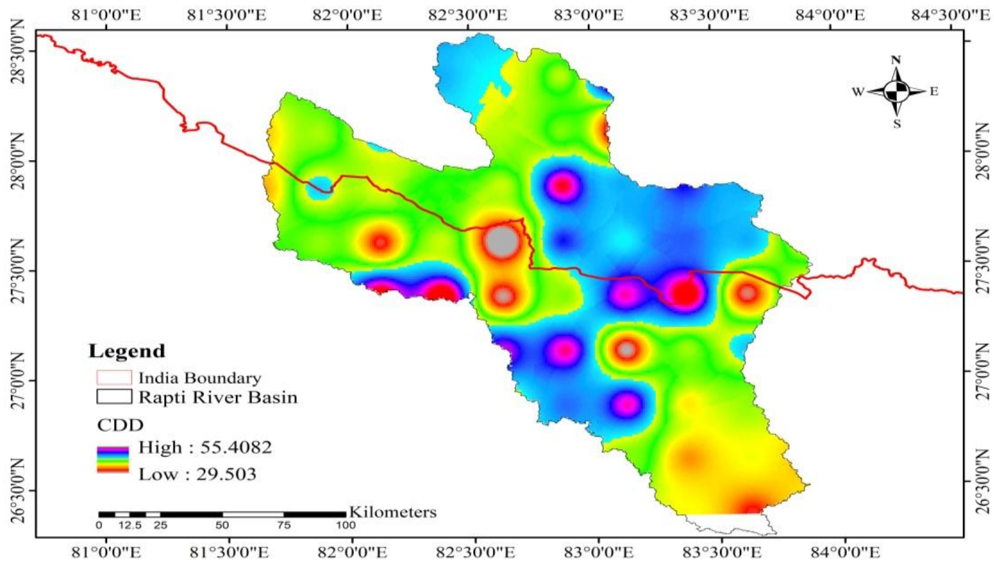


**Figure 3: Consecutive Dry Days (CDD) atACCESS-CM2 Model for 2˚**

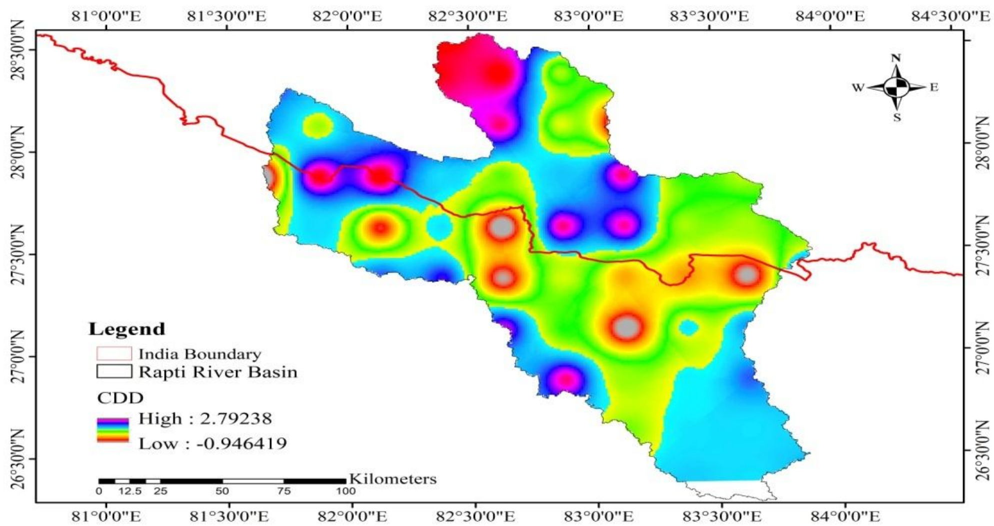


**Figure 4: Consecutive Dry Days (CDD) atACCESS-CM2Modelfor3˚**

## 3.2 Annual Trend Analysis of Extreme Precipitation Indices

During the period of 2020-2031 at 1.5˚C, under Model ACCESS-CM2 (M1), ssp585, the Consecutive Dry Days (CDD) show a notable decrease in trend, with a reduction of -0.34 (-0.45), corresponding to a decrease in slope of -1.08 days per year. In contrast, for Model ACCESS-ESM1-5 (M2), there is a more significant decrease in trend, amounting to -2.90 (-1.43), resulting in a decrease in slope of -6.49 days per year.

Under Model ACCESS-CM2, ssp585, at 2˚C (2032-2050),there is a notable decrease in trend for Consecutive Dry Days (CDD) of -0.08 (-0.93), resulting in a decrease in slope of -8.07 days per year.

At 3˚C (2051-2060), under Model M1, ssp585, there is a substantial decrease in trend for Consecutive Dry Days (CDD) of -1.59 (-1.45), resulting in a decrease in slope of -3.42 days per year.

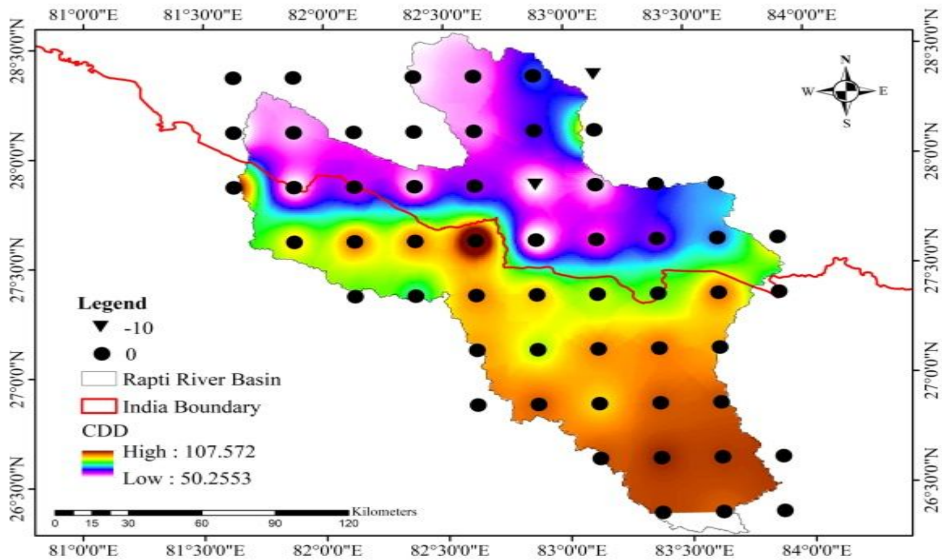


**Figure 5: Trends of Consecutive Dry Days (CDD) at ACCESS-CM2 Model for 1.5˚**

**Here, # = -10 indicate a decrease in the number of Consecutive Dry Days by 10 days.**

**l = 0 indicates no change in the number of Consecutive Dry Days**

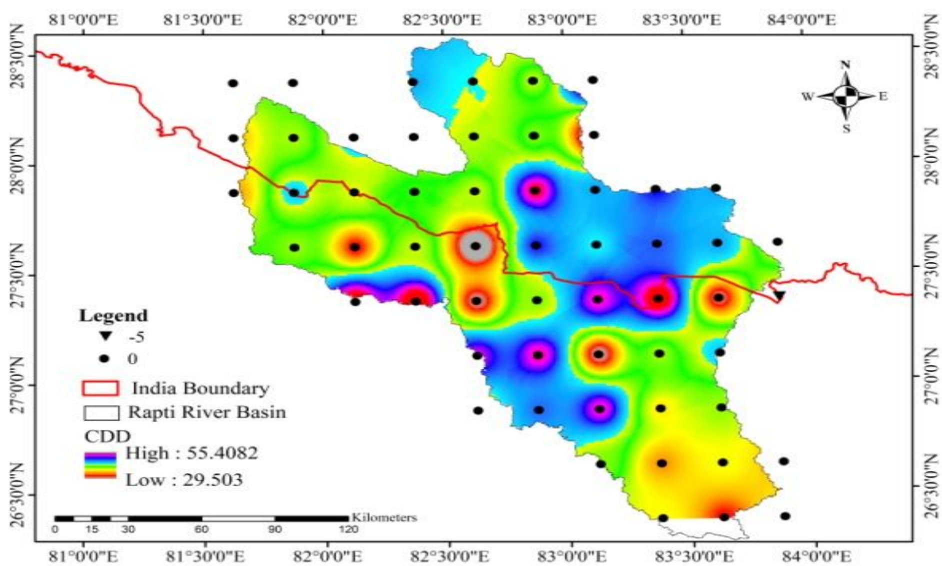


**Figure 6: Trends of Consecutive Dry Days (CDD) atACCESS-CM2 Model for 2˚**

Here, # **= -5 indicate a decrease in the number of Consecutive Dry Days by 5 days.**

**l = 0 indicates no change in the number of Consecutive Dry Days**

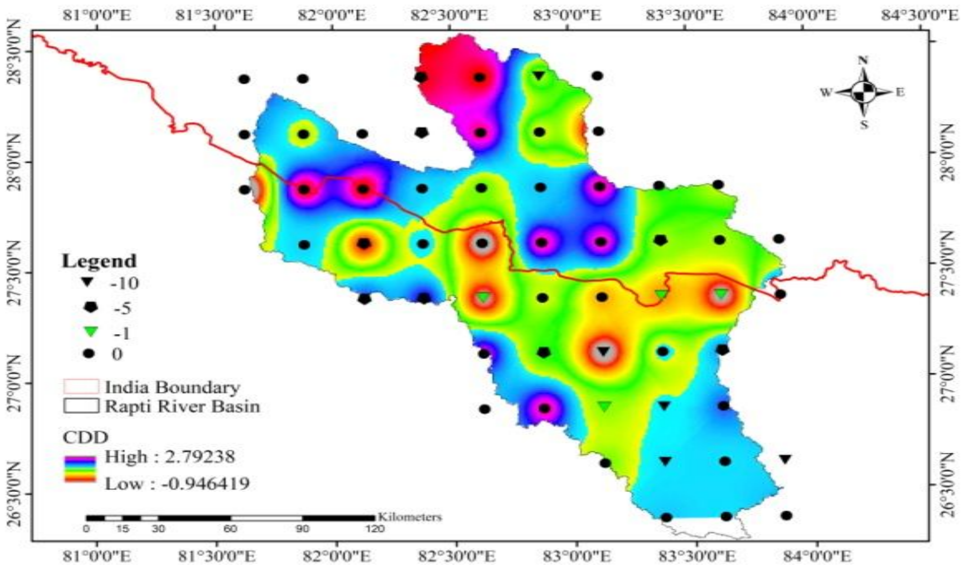


**Figure 7: Trends of Consecutive Dry Days (CDD) at ACCESS-CM2 Model for 3˚**

**Here,**

**i = 0 indicates no change in the number of Consecutive Dry Days**

**# = -1 indicate a decrease in the number of Consecutive Dry Days by 1 day**

**% = -5 Indicate a decrease in the number of Consecutive Dry Days by 5 days**

## 4. CONCLUSION

This study provides a comprehensive analysis of extreme precipitation events in the Rapti River Basin, India, utilizing multiple models and indices to evaluate both historical and projected trends.

- The findings highlight significant variations in the trends and magnitudes of Consecutive Dry Days (CDD) across different global warming levels of 1.5˚C, 2˚C, and 3˚C.
- The analysis indicates that the Rapti River Basin is experiencing significant changes in precipitation patterns, driven by climate change. Under the various models and scenarios analyzed, the results show both increases and decreases in the trends of CDD with notable variations in the slopes, reflecting the complex and dynamic nature of the basin's hydrological response to global warming.
- Specifically, at 1.5˚C, there is a decreasing trend in CDD, suggesting variability in dry spells. At 2˚C, the models project a further decrease in CDD, indicating a shift towards more frequent wet spells. At 3˚C, while some models show a continued decrease in CDD, others indicate a significant increase in CDD, implying potential risks of prolonged wet periods and associated flood events.
- These findings underscore the critical need for adaptive water resource management strategies in the Rapti River Basin. The projected changes in extreme precipitation events, including increased frequency and intensity of both droughts and floods, pose significant challenges to agriculture, infrastructure, and livelihoods in the region.

This research emphasizes the importance of continuous monitoring and assessment of precipitation trends using advanced climate models and indices. Policymakers and stakeholders must prioritize the development of robust adaptation and mitigation strategies to address the impacts of climate change on the Rapti River Basin, ensuring sustainable water resource management and resilience of the local communities to future climatic extremes.

## CONSENT

All authors declare that 'written informed consent was obtained from the patient (or other approved parties) for publication of this case report and accompanying images. A copy of the written consent is available for review by the Editorial office/Chief Editor/Editorial Board members of this journal.

**Disclaimer (Artificial intelligence)**

Option 1:

Author(s) hereby declare that NO generative AI technologies such as Large Language Models (ChatGPT, COPILOT, etc) and text-to-image generators have been used during writing or editing of manuscripts.

I did not use AI for any text to image generators.

Option 2:

Author(s) hereby declare that generative AI technologies such as Large Language Models, etc have been used during writing or editing of manuscripts. This explanation will include the name, version, model, and source of the generative AI technology and as well as all input prompts provided to the generative AI technology

Details of the AI usage are given below:

1.

2.

3.

**REFRENCES**


1. IPCC. (2014). Climate Change 2014: Synthesis Report. Contribution of Working Groups I, II, and III to the Fifth Assessment Report of the Intergovernmental Panel on Climate Change. Geneva, Switzerland: IPCC.
2. Solomon, S., Manning, M., Marquis, M. & Qin, D. 2007 Climate Change 2007 - The Physical Science Basis: Working Group I Contribution to the Fourth Assessment Report of the IPCC, Vol. 4. Cambridge University Press, Cambridge and New York, p. 1009.
3. Gu, X., Zhang, Q., Singh, V. P. & Shi, P. 2017 Changes in magnitude and frequency of heavy precipitation across China and its potential links to summer temperature. Journal of Hydrology 547, 718–731. https://doi.org/10.1016/j.jhydrol.2017.02.041.
4. Zhang, K., Yao, Y., Qian, X. & Wang, J. 2019 various characteristics of precipitation concentration index and its cause analysis in China between 1960 and 2016. International Journal of Climatology 39(12), 4648–4658. https://doi.org/10.1002/ joc.6092.
5. Neitsch, S. L., et al. (2011). Soil and Water Assessment Tool Theoretical Documentation Version 2009. Texas Water Resources Institute.
6. Kumar, R. 2019 Flood frequency analysis of the Rapti River Basin using log Pearson type-III and Gumbel extreme value-1 methods. Journal of the Geological Society of India 94(5), 480–484. https://doi.org/10.1007/s12594-019-1344-0.
7. Central Water Commission. (2014). "Rapti Basin Report." Ministry of Water Resources, Government of India.
8. Chalise, S. R., & Khanal, N. R. (2001). "Hydrology of Nepal: Proceedings of the Workshop on Hydrology and Meteorology." ICIMOD.

9. Sharma, R. H., & Shakya, N. M. (2006). "Hydrological changes and its impact on water resources of Bagmati watershed, Nepal." *Journal of Hydrology*, 327(3-4), 315-322.
10. Bhattarai, R., & Acharya, K. (2018). "Climate change impacts on hydrology and water resources of the Upper Bagmati River Basin, Nepal." *Climate*, 6(3), 63.
11. ICIMOD. (2011). "Climate Change in the Himalayas: Current State of Knowledge." International Centre for Integrated Mountain Development.
12. Aadhar, S. and Mishra, V., 2020. On the projected decline in droughts over South Asia in CMIP6 multimodel ensemble. *Journal of Geophysical Research: Atmospheres*, *125*(20), p.e2020JD033587.
13. Mann HB. 1945. Nonparametric tests against trend, Econometrica 13: 245–259.
14. Kendall, M.G. (1975) Rank Correlation Methods. London: Charles Griffin.
15. Yue S, Pilon P, Phinney B, Cavadias G. 2002. The influence of autocorrelation on the ability to detect trend in hydrological series. Hydrol. Process. 16(9): 1807–1829.
16. Some'e, B.S., Ezani, A. and Tabari, H., 2012. Spatiotemporal trends and change point of precipitation in Iran. *Atmospheric research*, *113*, pp.1-12.
17. Gidden, M.J., Riahi, K., Smith, S.J., Fujimori, S., Luderer, G., Kriegler, E., van Vuuren, D.P., van den Berg, M., Feng, L., Klein, D., Calvin, K., Doelman, J.C., Frank, S., Fricko, O., Harmsen, M., Hasegawa, T., Havlik, P., Hilaire, J., Hoesly, R., Horing, J., Popp, A., Stehfest, E., Takahashi, K., 2019. Global emissions pathways under different socioeconomic scenarios for use in CMIP6: a dataset of harmonized emissions trajectories through the end of the century. Geoscientific Model Development 12, 1443–1475. https://doi.org/10.5194/gmd-12-1443-2019.
18. O'Neill, B.C., Kriegler, E., Ebi, K.L., Kemp-Benedict, E., Riahi, K., Rothman, D.S., van Ruijven, B.J., van Vuuren, D.P., Birkmann, J., Kok, K., Levy, M., Solecki, W., 2017. The roads ahead: Narratives for shared socioeconomic pathways describing world futures in the 21st century. Global Environmental Change 42, 169–180. https://doi.org/10.1016/j.gloenvcha.2015.01.004
19. Donat MG, Alexander LV, Yang H, Durre I, Vose R, Dunn RJH, Willett KM, Aguilar E, Brunet M, Caesar J, Hewitson B, Jack C, Klein Tank AMG, Kruger AC, Marengo J, Peterson TC, Renom M, Oria Rojas C, Rusticucci M, Salinger J, Elrayah AS, Sekele SS, Srivastava AK, Trewin B, Villarroel C, Vincent LA, Zhai P, Zhang X, Kitching S. 2013,"Updated analyses of temperature and precipitation extreme indices since the beginning of the twentieth century", the hadex2 dataset. J. Geophys. Res. Atmos. 118(5): 2098–2118.
20. Alexander, L.V., Fowler, H.J., Bador, M., Behrangi, A., Donat, M.G., Dunn, R., Funk, C., Goldie, J., Lewis, E., Rogé, M. and Seneviratne, S.I., 2019. On the use of indices to study extreme precipitation on sub-daily and daily timescales. *Environmental Research Letters*, *14*(12), p.125008.
21. Liang K, Liu S, Bai P, Nie R. The Yellow River basin becomes wetter or drier? The case as indicated by mean precipitation and extremes during 1961–2012. Theoretical and Applied Climatology. 2015 Feb;119:701-22.
22. Santos CA, BrasilNeto RM, da Silva RM, Passos JS. Integrated spatiotemporal trends using TRMM 3B42 data for the Upper São Francisco River basin, Brazil. Environmental monitoring and assessment. 2018 Mar;190:1-20.
23.